GDCh Research Article Angewandte International Edition Chemie www.angewandte.org

Check for updates

How to cite: *Angew. Chem. Int. Ed.* **2026**, *65*, e20887
doi.org/10.1002/anie.202520887

On-Surface Synthesis

Substrate-Selective Temperature-Controlled Synthesis of Thiophene Derivatives at Interfaces

Elena Pérez-Elvira[+], *Ana Barragán*[+]*, *Diego J. Vicent*[+], *Óscar Jóver*, *Aurelio Gallardo*, *Alba García-Frutos*, *Lenka Černa*, *Koen Lauwaet*, *José Santos*, *Josefina Perles*, *José M. Gallego*, *Rodolfo Miranda*, *José I. Urgel*, *Jonas Björk*,* *Marco Di Giovannantonio*,* *Nazario Martín*,* *and David Écija**

Abstract: The temperature-controlled transformation of organic molecules at interfaces is an incipient yet powerful strategy for tailoring their structural and physico-chemical properties. In this study, we investigate the substrate- and thermal-selective reactions of bis(3,4-thiophene-fused)tetrabromo-*p*-benzoquinodimethane molecule (**1**), focusing on its behavior at distinct coinage metal interfaces, namely Au(111) and Ag(111). Combining scanning probe microscopy and theory, we demonstrate that its sequential transformations are highly dependent on the substrate material and the specific reaction temperatures. When a benzodithiophene precursor, endowed with = CBr_2 units, is deposited under ultra-high vacuum (UHV) conditions on both substrates held at room temperature (RT), or annealed to 100 °C in the case of Au(111), a self-assembly is formed comprising 1D covalent polymers achieved through debromination and homocoupling, which are aligned in a parallel fashion thanks to supramolecular interactions, giving rise to a 2D supramolecular polymer. However, when the substrate is held at or above 175 °C during deposition, the molecular precursors (**1**) undergo substrate-specific intramolecular reactions. On Au(111), a major transformation into pentalenodithiophene species is observed, concomitant with the formation of benzotrithiophene. On Ag(111), instead, pentalenodithiophene species are precluded. These findings highlight the importance of substrate selection and temperature control in enabling precise molecular transformations at the nanoscale.

Introduction

Over the past two decades, on-surface covalent synthesis under ultra-high vacuum (UHV) conditions, frequently termed "on-surface synthesis", has emerged as a powerful strategy for designing unprecedent molecular species, involving unique reaction pathways, while at the same time, allowing the capabilities of scanning probe microscopies for structural, electronic, and magnetic characterization at the atomic scale.[1–4] Notable examples of synthesis on metallic surfaces include nanographenes,[5–10] the formation of 1D nanowires,[2,11–14] the engineering of quasi-1D conjugated ladder polymers (graphene nanoribbons),[15–18] or even the atomically precise fabrication of 2D covalent networks.[19–21]

[*] E. Pérez-Elvira[+], Dr. A. Barragán[+], Dr. A. Gallardo, A. García-Frutos, L. Černa, Dr. K. Lauwaet, Prof. R. Miranda, Dr. J. I. Urgel, Prof. N. Martín, Prof. D. Écija
IMDEA Nanoscience, C/ Faraday 9, Campus De Cantoblanco, Madrid 28049, Spain
E-mail: ana.barragan@imdea.org
nazmar@ucm.es
david.ecija@imdea.org

Dr. D. J. Vicent[+], Dr. J. Santos, Prof. N. Martín
Departamento De Química Orgánica, Facultad De Ciencias Químicas, Universidad Complutense, Madrid 28040, Spain

Dr. Ó. Jóver, Dr. M. Di Giovannantonio
CNR-Istituto Di Struttura della Materia (CNR-ISM), Roma 00133, Italy
E-mail: marco.digiovannantonio@cnr.it

Dr. J. Perles
Laboratorio DRX Monocristal, SIdI, Universidad Autónoma de Madrid, Madrid 28049, Spain

Dr. J. M. Gallego
Instituto De Ciencia de Materiales de Madrid (ICMM), CSIC, Madrid 28049, Spain

Dr. J. I. Urgel, Prof. D. Écija
Unidad De Nanomateriales Avanzados, IMDEA Nanoscience, Unidad asociada Al CSIC Por El ICMM, Madrid 28049, Spain

Prof. J. Björk
Materials Design Division, Department of Physics, Chemistry and Biology (IFM), Linköping University, Linköping SE-581 83, Sweden
E-mail: jonas.bjork@liu.se

[+] These authors contributed equally to this work.

Additional supporting information can be found online in the Supporting Information section

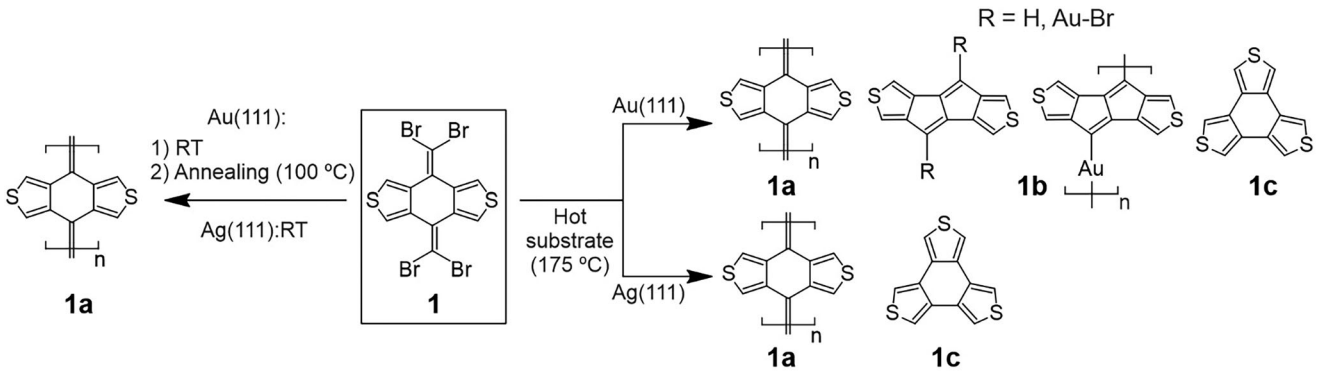

Scheme 1. Reactivity of precursor **1** on Au(111) and Ag(111) under distinct thermal annealing procedures.

A key aspect of the emerging field of on-surface synthesis is understanding the various factors that govern chemical reactivity, including the choice of substrate, molecular backbone, functional groups, and external stimuli such as thermal annealing, light, or electron beam irradiation.[1,3] Remarkably, most successful experiments in terms of novel reaction mechanisms and reaction products involve sublimating precursor molecules onto a substrate at room temperature (RT), followed by annealing to a specific temperature. Driven by such success, in the last decade a growing interest is set on elucidating thermally selective reactions, specifically how the substrate temperature during molecular deposition can steer distinct reaction pathways.[3,22–24]

Thiophene-containing compounds have garnered significant attention due to their versatile applications across various fields.[25–31] In material science, thiophene-based compounds are pivotal in the development of organic semiconductors, which are essential for organic photovoltaics (OPVs), organic field-effect transistors (OFETs), and organic light-emitting diodes (OLEDs).[27,29,32] In medicinal chemistry, thiophene derivatives are known for diverse pharmacological activities, including antimicrobial, anti-inflammatory, anticonvulsant, antifungal, and anticancer properties. Several marketed drugs, such as Thiophenfurin, Teniposide, and Cefoxitin, incorporate thiophene nuclei, underscoring their therapeutic importance.[30] Altogether, the unique electronic properties, chemical versatility, and structural stability of thiophene derivatives make them indispensable in both medicinal and material sciences, driving ongoing research and development in these areas.

Driven by such importance, the chemistry of thiophene derivatives on metal surfaces has been broadly explored, generally illustrating the preservation of thiophene units on Au(111) or Ag(111),[33–36] while demonstrating desulfurization and intramolecular reactivity on Cu(111) or Ni(111).[37–40]

Inspired by the relevance of this family of compounds, the potential of thiophene to induce intramolecular reactivity at metal interfaces, and by our recent discovery of intramolecular rearrangements[4,10,39,41–47] using the *gem*-dibromovinylene ($C{=}CBr_2$) functional group on both Au(111) and Ag(111), in this work we report the synthesis and on-surface reactivity of precursor **1** (see Scheme 1). This compound is a benzodithiophene derivative endowed with two $=CBr_2$ groups, each one of them placed at the apex of a six-membered ring, enabling the exploration of competing intermolecular and intramolecular reactions.

Our comprehensive scanning tunneling and non-contact atomic force microscopy (STM/nc-AFM) studies under UHV conditions, complemented by X-ray photoelectron spectroscopy (XPS) and density functional theory (DFT) calculations, reveal that the deposition of a submonolayer coverage of **1** on pristine Ag(111) held at RT gives rise to the formation of 1D molecular wires (**1a**). The same polymerization is found on Au(111) after subsequent annealing to 100 °C. In contrast, sublimation of the precursor on a hot Au(111) or Ag(111) substrate held at 175 °C results in distinct reaction products. On Au(111), the reaction predominantly yields pentalenodithiophene derivatives (**1b**), with minor residual trithiophene species (**1c**). However, on the more reactive Ag(111), the formation of pentalenodithiophene (**1b**) is inhibited, and trithiophene species (**1c**) emerge as the main product. Notably, species **1a** can still be found in small regions on both substrates. Our mechanistic study on Ag(111) indicates that metal adatoms play a key role by attacking the precursor, leading to the formation of diradical thiophenes that diffuse across the surface and couple into trithiophene species (**1c**).

Results and Discussion

Molecule **1** was synthesized following the procedure described in the Supporting Information (cf. Figures S1–S6), by functionalizing 4*H*,8*H*-benzo[1,2-*c*:4,5-*c*']dithiophene-4,8-dione with two $=CBr_2$ moieties. Recently, *gem*-dibromides were found to be versatile for the on-surface synthesis of carbon nanomaterials.[11–14,18,23,48–51] In particular, it has been reported that the *gem*-dibromovinylene functional group can steer polymerization when the precursor species are deposited at RT and subsequently annealed,[11–14,18,49,50] or afford intramolecular rearrangement when the precursor is adsorbed on a hot substrate.[23] To elucidate the dominant reaction pathway for this thiophene derivative on Au(111) and Ag(111), we inspected both scenarios.

In the first scenario, the deposition of a submonolayer coverage of **1** on Au(111) held at RT gives rise to supramolecular

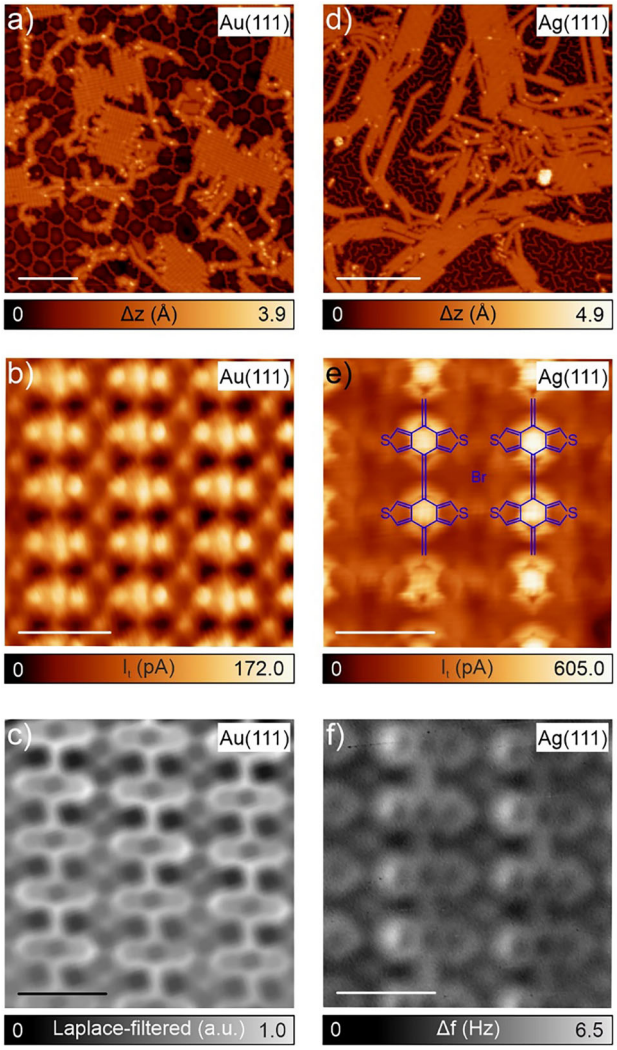

Figure 1. On-surface synthesis of 1D cumulene-bridged benzodithiophene polymers **1a** on Au(111) and Ag(111). a) and d) Overview STM images after deposition of **1** on Au(111) and Ag(111) substrates at RT, respectively, and post annealing at 100 °C on Au(111). $V_b = 0.2$ V, $I_t = 50$ pA, scale bar: 10 nm, and $V_b = 0.5$ V, $I_t = 10$ pA, scale bar: 10 nm, respectively. b) and e) Zoom-in constant-height STM images of the obtained 1D covalent wires on top of Au(111) and Ag(111) substrates, respectively. Open feedback parameters: Z-offset: 20 pm below STM set point (5 mV, 50 pA), and Z-offset: 17 pm above STM set point (5 mV, 50 pA), respectively. Scale bar: 1 nm. c) and f) Corresponding Laplace-filtered and original nc-AFM images, respectively. Z-offset: 15 pm below STM set point (5 mV, 50 pA), and Z-offset: 35 pm below STM set point (5 mV, 50 pA), respectively. Scale bar: 1 nm.

patches (cf. Figure S7). Further annealing to 100 °C induces the formation of linear 1D-chains organized into 2D patches, surrounded by Br-based nanostructures (cf. Figure 1a). High-resolution constant-height STM and constant-height frequency-shift nc-AFM images acquired with a CO tip[52,53] allow to elucidate the nature of such patches. They can be rationalized as a 2D hybrid nanostructure, comprising on a first level of hierarchy 1D covalent wires based on benzodithiophene monomers linked by cumulene-bridges (**1a**) (cf. Figure 1b,c). At a second hierarchical level, the 1D wires are aligned in a parallel fashion, resulting in a 2D supramolecular nanoarchitecture based on 1D chains, which are held together by H•••Br interactions between the peripheral hydrogen atoms from the thiophene rings and interstitial bromine atoms. In addition, the thiophene moieties are placed face to face, reinforcing the formation of 2D patches with S•••S supramolecular interactions. High resolution nc-AFM images reveal an experimental S•••S distance of ~3.5 Å, which is in good agreement with the simulated distance of ~3.7 Å (cf. Figure S9).

Reproducing the same protocol on Ag(111) affords the formation of the same 2D hybrid nanoarchitecture already at RT (cf. Figure 1d–f), and additionally yields some isolated molecular wires (cf. Figure S8). Our rationalization is corroborated by the simulation of the model by DFT calculations (cf. Figure S9). A stepwise annealing at temperatures beyond 175 °C disassembles the 2D network and induces the formation of amorphous wires featuring ladder-like oligomeric segments on Au(111) (cf. Figure S10), whereas on Ag(111) it leads to the formation of amorphous wires above 200 °C (cf. Figure S11).

In the alternative sample preparation procedure, the sublimation of a submonolayer coverage of **1** on Au(111) held at 175 °C results in markedly different outcomes than those described above. In addition to the linear chains, the surface now features discrete molecular species surrounded by interstitial bromine atoms (cf. Figure 2a). The main products are pentaleno[1,2-*c*:4,5-*c*″]dithiophene species (**1b**) (~60%), either passivated by -H or by Au-Br (cf. Figure 2a,b) or featuring organometallic oligomers (cf. Figure 2c,d). This signals the intramolecular rearrangement of the precursor upon thermal activation of the *gem*-dibromovinylene functional group, as previously encountered for acene and sumanene species on Au(111).[23,24] It is important to highlight that the antiaromatic pentalene-containing molecule **1b** (R=H) has not previously been synthesized in solution, probably due to its poor stability, and only a few derivatives of **1b** (R≠H) have been successfully prepared.[54,55] Notably, the presence of benzo[1,2-*c*:3,4-*c*″:5,6-*c*‴″]trithiophene compound (**1c**) is also detected (see discussion below), though as a minor species (~20%). This reaction product suggests the possible rupture of C–C bonds in the precursor **1** to create thiophene radicals able to diffuse and react on the surface to form benzotrithiophene species.

Thus, in principle, a more reactive surface than Au(111), for instance Ag(111), could alter the proportion of pentalenodithiophene (**1b**) versus trithiophene (**1c**) reaction products. In fact, the deposition of a submonolayer coverage of **1** on Ag(111) held at 175 °C results in the dominant formation of trithiophene species (**1c**) with a yield of ~40%, while the remaining surface is populated by **1a** linear chains (~20%) and defective species (cf. Figures 2e and S12). Importantly, the synthesis of pentalenodithiophene species (**1b**) is blocked. High-resolution constant-height STM images display the benzotrithiophene species, both on Au(111) and Ag(111), as three bright protrusions assigned to intact thiophenes, covalently assembled in a three-fold fashion (cf. Figures 2b and e–g, respectively). Submolecular insights of the reaction product are obtained on Ag(111) with constant-height

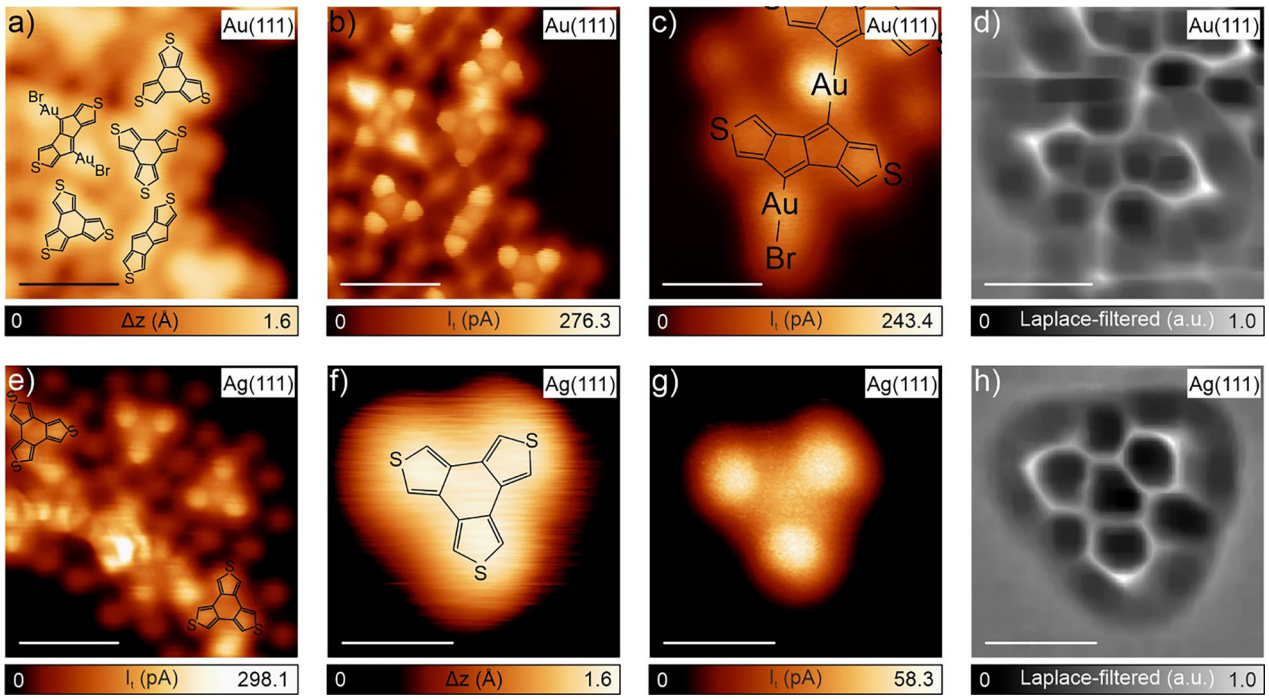

Figure 2. On-surface synthesis of trithiophene on Au(111) and Ag(111) by depositing precursor **1** onto pre-heated substrates at 175 °C. a) and b) Constant-current and constant-height STM images on Au(111) revealing the presence of species **1b**, either passivated by H or by Au-Br, and species **1c**. $V_b = 0.5$ V, $I_t = 50$ pA, scale bar: 1 nm, and $V_b = 5$ mV, $I_t = 50$ pA, z-offset = 20 pm bellow the STM set point, scale bar: 1 nm, respectively. c) and d) Constant-height STM image and Laplace-filtered nc-AFM image of specie **1b** as an organometallic, also observed in the reaction. $V_b = 5$ mV, $I_t = 50$ pA, z-offset = 50 pm above the STM set point, scale bar: 1 nm. e) Constant-height STM image of the reaction on Ag(111) revealing the presence of species **1c** and some defective species. $V_b = 5$ mV, $I_t = 50$ pA, z-offset = 100 pm above the STM set point, scale bar: 1 nm. f) and g) Constant-current and constant-height STM images of an individual benzotrithiophene species **1c**. $V_b = 0.5$ V, $I_t = 50$ pA, scale bar: 0.5 nm, and $V_b = 5$ mV, $I_t = 50$ pA, z-offset = 160 pm above the STM set point, scale bar: 0.5 nm, respectively. h) Laplace-filtered nc-AFM image of panel g. Z-offset: 160 pm above STM set point (5 mV, 50 pA), scale bar: 0.5 nm.

nc-AFM, allowing us to unambiguously discern the species, assigning them to benzotrithiophene. Notably, the match between experimental and simulated STM and nc-AFM images (cf. Figures 2f–h and S13) is excellent, being the sulfur atom in nc-AFM observed with a slightly brighter contrast.

Intrigued by the preservation of thiophene moieties, we performed XPS experiments on selected samples to confirm the integrity of such moieties and the presence of sulfur atoms in the same thiophene chemical environment as in the pristine molecular precursors. We investigated the molecular adsorption and transformation on Ag(111).

Here, we compared three samples; where **1** was deposited at RT, subsequently annealed to 175 °C, and deposited on the substrate held at 175 °C. The first sample is representative of the 2D supramolecular nanoarchitecture, the second of such nanoarchitecture at higher T, but still preserving the polymer, and the third showcases the benzotrithiophene phase, respectively. Figure 3 shows the XPS spectra at the S 2p core level for these samples. After depositing **1** on Ag(111) at RT, a doublet is observed in the S 2p XPS spectrum (cf. Figure 3a). This signal corresponds to the sulfur atoms in the pristine thiophene rings that appear in the 1D polymers (cf. Figures 1d–f). Annealing this surface to 175 °C (Figure 3b) produces the appearance of a second doublet at lower binding energy (shifted by 2.3 eV compared to the main doublet). This signal amounts to 29% of the total intensity and we attribute it to the interaction of some of the sulfur atoms with Ag adatoms, which are presumably generated at this higher annealing temperature and are stabilized at the sulfur sites after diffusing on the surface. The main doublet remains at its energy position, indicating that the majority of thiophenes are unaltered as compared to the RT phase. When **1** is deposited on a Ag(111) surface held at 175 °C (Figure 3c), a main doublet representative of unperturbed thiophene species is detected, alongside with a small signal arising from S–Ag interactions (12% of the total signal). Notably, the detection of the main S 2p signal in its pristine chemical state confirms that thiophene species are still present on the surface, hence we can confirm the achievement of benzotrithiophene compounds.

To investigate the reaction mechanism responsible for the synthesis of benzotrithiophene, we performed DFT-based transition state theory calculations, exploring distinct synthetic scenarios based on our scanning probe microscopy and XPS results. The most plausible pathway involves an Ag adatom assisting the detachment of thiophene species from precursor **1** followed by their diffusion and aggregation to form the three-membered benzotrithiophene (**1c**) final product. During the detachment of the thiophene units from **1** (Figure S14), the carbon atoms involved in the first bond scission increasingly interact with the substrate, forming intermediate **S1″**. In this intermediate, one carbon atom from

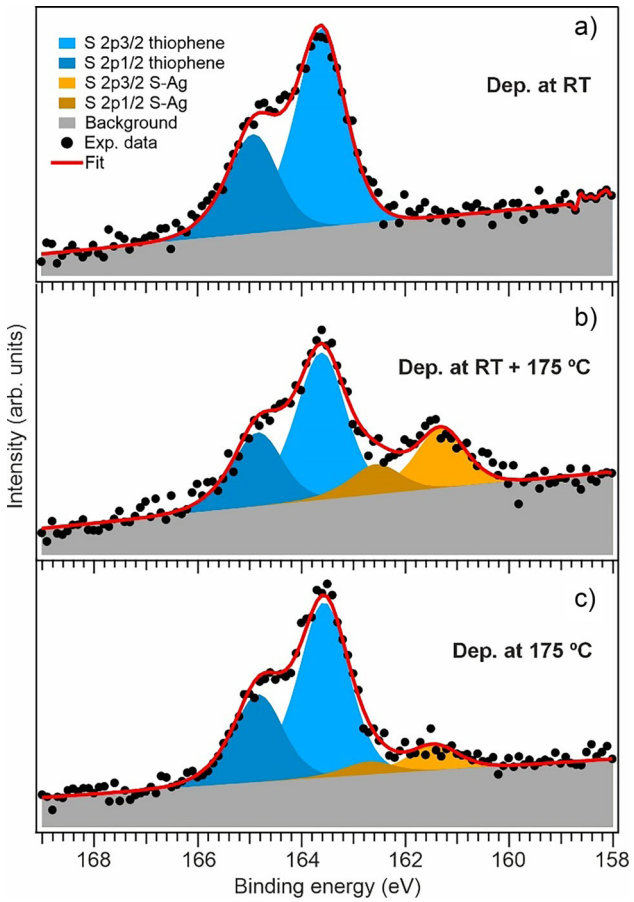

Figure 3. XPS data indicating the preservation of thiophene moieties after depositing precursor **1** on Ag(111) in different conditions, reported in each panel: a) deposition at RT, b) deposition at RT and subsequent annealing at 175 °C, and c) deposition on the substrate held at 175 °C, respectively.

the thiophene unit is detached from **1** and is stabilized on the surface by an Ag adatom. A second Ag adatom then engages with the remaining carbon atom still bound to the precursor **1**, promoting the final C─C bond cleavage and fully releasing the thiophene unit.

Concerning the formation of benzotrithiophene species from thiophene moieties, Figure 4 illustrates the proposed mechanism. In this model, two and three thiophene units aggregate around an Ag atom on Ag(111), forming two- and three-fold covalently bonded structures, allowing a direct comparison of their thermodynamic tendencies. For this evaluation, we assumed that the independent thiophene units had been previously isolated from precursor **1**. Of two tentative mechanisms considered (cf. Figure S14), the most likely is a two-step process, with activation energies of 1.69 and 2.19 eV, and a net energy cost of 1.32 eV per newly formed thiophene unit.

Accounting for this energy cost, two-fold bonded thiophene formation is endothermic (reaction energy of 1.16 eV), in contrast to benzotrithiophene (**1c**), which forms exothermically (reaction energy of −2.70 eV).

To understand these energy differences, we considered the detailed reaction pathways leading to two- and three-fold bonded thiophene structures. For the reaction of two thiophene units in the presence of an adatom (cf. Figure 4a), the molecules undergo a two-step process. First, they form a covalent bond (activation energy 1.01 eV, releasing 1.32 eV). Then, a second bond is established (activation energy 1.34 eV) yielding a cyclobutadithiophene species 1.48 eV lower in energy than the separate thiophene counterparts. Considering the 2.64 eV energy cost to generate the two thiophenes, the overall process is endothermic.

For the reaction of three thiophene units, the system follows the reaction depicted in Figure 4b. First, two thiophene units covalently couple, analogously to the first step of the dimerization. The rate-limiting step, corresponding to the covalent bond formation from S4' to S5', has an activation energy of 1.21 eV. Upon detachment from the Ag adatom, only a small energy barrier of 0.66 eV separates the trimeric complex from the final state S6', which lies 6.66 eV below the three separated thiophene units. Accounting for the 3.96 eV energy cost to generate the three thiophene units, the overall process is exothermic, with an energy release of 2.70 eV.

These calculations indicate that trimerization is both kinetically and thermodynamically preferred over dimerization, consistent with our experimental findings that benzotrithiophene (**1c**) predominates, and that cyclobutadithiophene is not detected.

Finally, we performed DFT simulations of the electronic structure of the products **1b** and **1c**, which reveal the closed-shell character of the species (Figure S15a). In addition, calculated NICS (0) signal at the centre of all the rings of each species, displays a very low antiaromaticity of the central ring of the benzotrithiophene compound (+2.7 ppm), and an enhanced aromaticity of its thiophene units (−11.8, −11.8, and −11.9 ppm) in comparison with pentalenodithiophene compound (−7.0 and −7.1 ppm, cf. Figure S15b).

Conclusions

In this study, we have explored the on-surface synthesis and reactivity of a *p*-benzoquinodithiophene derivative bearing two $=CBr_2$ moieties (**1**), revealing the influence of substrate type and deposition temperature on reaction pathways. Our results highlight the potential of thermally selective reactions at metal interfaces, with distinct outcomes observed on Au(111) and Ag(111). The deposition of the precursor at RT followed by annealing to 100 °C on Au(111) or directly at RT on Ag(111) led to the formation of 1D covalent molecular wires on both substrates, self-assembled into a supramolecular architecture benefiting from H•••Br and S•••S interactions. However, sublimation onto the same substrates held at 175 °C unveiled substrate-specific reaction pathways. On Au(111), predominantly pentalenodithiophene derivatives (**1b**) were obtained, with only minor amounts of benzotrithiophene (**1c**) and covalent wires. In contrast, the more reactive Ag(111) substrate inhibited the formation of pentalenodithiophene species and favored the generation of benzotrithiophene, alongside the 1D polymers. Mechanistic insights revealed that the reactivity on Ag(111) was driven by the attack

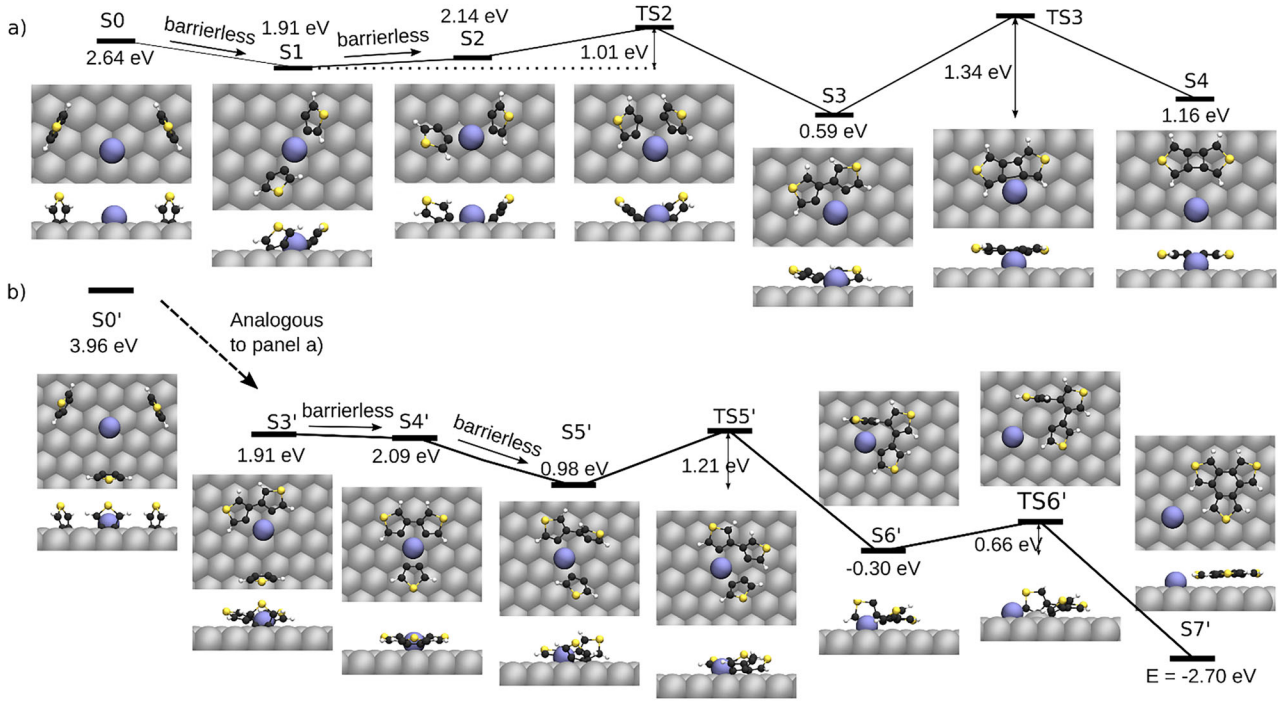

Figure 4. DFT-calculated pathway for transforming precursor **1** into cyclobutadithiophene and benzotrithiophene on a Ag(111) substrate. Proposed hypothetic mechanism for the creation of a) cyclobutadithiophene and b) benzotrithiophene (species **1c**). The total energies are referred to the cost of generating the necessary thiophene units (cf. Figure S14). The Ag adatom that mediates the reaction is depicted in blue for clarity. Ag, S, C, and H atoms are depicted in gray, yellow, black, and white, respectively.

of metal adatoms to C─C bonds of the precursor, which facilitated the formation of diradical thiophene species. These intermediates diffused across the surface and reacted to yield benzotrithiophene as the primary product.

Our findings reveal the critical role of substrate temperature and reactivity in determining reaction pathways and product selectivity. The distinct on-surface synthesis behaviors on Au(111) and Ag(111) exemplify how substrate properties can be leveraged to direct molecular reactivity at interfaces. This study advances the understanding of organic chemistry and on-surface synthesis, demonstrating the versatility of thiophene chemistry. In addition, our results highlight that strategically tuning substrate and thermal parameters, new opportunities arise for the design of tailored molecular compounds with potential applications in organic optoelectronics and materials science.

Suppporting Information

The authors have cited additional references within the Supporting Information.[56–68]

Acknowledgements

The authors acknowledge to several funding organizations for their financial support. The authors thank funding from Spanish State Research Agency (AEI: PID2019-108532GB-I00, PID2020-114653RB-I00, PID2022-136961NB-I00, PID2023-146373OB-I00); and QUIMTRONIC-CM Y2018/NMT-4783, the "(MAD2D-CM)-IMDEA-Nanociencia" and "(MAD2D-CM)-UCM" projects funded by Comunidad de Madrid, by the Recovery, Transformation and Resilience Plan, and by NextGenerationEU from the European Union. IMDEA Nanociencia is appreciative of support from the "Severo Ochoa" Programme for Centers of Excellence in R&D (CEX2020-001039-S). A.B. and A.G. acknowledge financial support from Juan de la Cierva program. A.G acknowledges the funding from IDEAL postdoctoral MSCA-cofund. J.B. acknowledges funding from Swedish Government Strategic Research Area in Materials Science on Advanced Functional Materials at Linköping University, Faculty Grant SFO-Mat-LiU 2009–00971. Computations were enabled by resources provided by the National Academic Infrastructure for Supercomputing in Sweden (NAISS), partially funded by the Swedish Research Council through grant agreement no. 2022–06725. J.I.U. acknowledges financial support from MCIU for the Ramón y Cajal program (RYC2022-037352-I). M.D.G. acknowledges the European Union, NextGenerationEU, Mission 4, Component 1, CUP B53D23013760006 and the Italian Ministry of University and Research (MUR) for the PRIN 2022 (project No. 2022JW8LHZ, ATYPICAL).

Conflict of Interests

The authors declare no conflict of interest.

Data Availability Statement

The data that support the findings of this study are available from the corresponding author upon reasonable request.

Keywords: Atomic force microscopy · On-surface synthesis · Scanning tunneling microscopy · Thiophene

[1] Q. Shen, H.-Y. Gao, H. Fuchs, *Nano Today* **2017**, *13*, 77–96, https://doi.org/10.1016/j.nantod.2017.02.007.

[2] Q. Sun, R. Zhang, J. Qiu, R. Liu, W. Xu, *Adv. Mater.* **2018**, *30*, 1705630, https://doi.org/10.1002/adma.201705630.

[3] S. Clair, D. G. de Oteyza, *Chem. Rev.* **2019**, *119*, 4717–4776, https://doi.org/10.1021/acs.chemrev.8b00601.

[4] B. Yang, B. Dong, L. Chi, *ACS Nano* **2020**, *14*, 6376–6382, https://doi.org/10.1021/acsnano.0c03766.

[5] Y. Gu, Z. Qiu, K. Müllen, *J. Am. Chem. Soc.* **2022**, *144*, 11499–11524, https://doi.org/10.1021/jacs.2c02491.

[6] K. Biswas, et al., *Angew. Chem. Int. Ed.* **2022**, *61*, e202114983.

[7] W. Zeng, J. Wu, *Chemistry (Weinheim An Der Bergstrasse, Germany)* **2021**, *7*, 358–386, https://doi.org/10.1016/j.chempr.2020.10.009.

[8] S. Song, J. Su, M. Telychko, J. Li, G. Li, Y. Li, C. Su, J. Wu, J. Lu, *Chem. Soc. Rev.* **2021**, *50*, 3238–3262, https://doi.org/10.1039/D0CS01060J.

[9] K. Biswas, D. Soler, S. Mishra, Q. Chen, X. Yao, A. Sánchez-Grande, K. Eimre, P. Mutombo, C. Martín-Fuentes, K. Lauwaet, J. M. Gallego, P. Ruffieux, C. A. Pignedoli, K. Müllen, R. Miranda, J. I. Urgel, A. Narita, R. Fasel, P. Jelínek, D. Écija, *J. Am. Chem. Soc.* **2023**, *145*, 2968–2974, https://doi.org/10.1021/jacs.2c11431.

[10] T. G. Lohr, J. I. Urgel, K. Eimre, J. Liu, M. Di Giovannantonio, S. Mishra, R. Berger, P. Ruffieux, C. A. Pignedoli, R. Fasel, X. Feng, *J. Am. Chem. Soc.* **2020**, *142*, 13565–13572, https://doi.org/10.1021/jacs.0c05668.

[11] A. Sánchez-Grande, B. De La Torre, J. Santos, B. Cirera, K. Lauwaet, T. Chutora, S. Edalatmanesh, P. Mutombo, J. Rosen, R. Zbořil, R. Miranda, J. Björk, P. Jelínek, N. Martín, D. Écija, *Angew. Chem. Int. Ed.* **2019**, *58*, 6559–6563, https://doi.org/10.1002/anie.201814154.

[12] B. Cirera, A. Sánchez-Grande, B. De La Torre, J. Santos, S. Edalatmanesh, E. Rodríguez-Sánchez, K. Lauwaet, B. Mallada, R. Zbořil, R. Miranda, O. Gröning, P. Jelínek, N. Martín, D. Ecija, *Nat. Nanotechnol.* **2020**, *15*, 437–443, https://doi.org/10.1038/s41565-020-0668-7.

[13] A. Sánchez-Grande, J. I. Urgel, I. García-Benito, J. Santos, K. Biswas, K. Lauwaet, J. M. Gallego, J. Rosen, R. Miranda, J. Björk, N. Martín, D. Écija, *Advancement of Science* **2022**, *9*, 2200407, https://doi.org/10.1002/advs.202200407.

[14] H. González-Herrero, J. I. Mendieta-Moreno, S. Edalatmanesh, J. Santos, N. Martín, D. Écija, B. d. l. Torre, P. Jelinek, *Adv. Mater.* **2021**, *33*, 2104495, https://doi.org/10.1002/adma.202104495.

[15] J. Cai, P. Ruffieux, R. Jaafar, M. Bieri, T. Braun, S. Blankenburg, M. Muoth, A. P. Seitsonen, M. Saleh, X. Feng, K. Müllen, R. Fasel, *Nature* **2010**, *466*, 470–473, https://doi.org/10.1038/nature09211.

[16] L. Talirz, P. Ruffieux, R. Fasel, *Adv. Mater.* **2016**, *28*, 6222–6231, https://doi.org/10.1002/adma.201505738.

[17] O. Gröning, S. Wang, X. Yao, C. A. Pignedoli, G. B. Barin, C. Daniels, A. Cupo, V. Meunier, X. Feng, A. Narita, K. Müllen, P. Ruffieux, R. Fasel, *Nature* **2018**, *560*, 209–213, https://doi.org/10.1038/s41586-018-0375-9.

[18] B. De La Torre, A. Matěj, A. Sánchez-Grande, B. Cirera, B. Mallada, E. Rodríguez-Sánchez, J. Santos, J. I. Mendieta-Moreno, S. Edalatmanesh, K. Lauwaet, M. Otyepka, M. Medveď, Á. Buendía, R. Miranda, N. Martín, P. Jelínek, D. Écija, *Nat. Commun.* **2020**, *11*, 4567, https://doi.org/10.1038/s41467-020-18371-2.

[19] C. Moreno, M. Vilas-Varela, B. Kretz, A. Garcia-Lekue, M. V. Costache, M. Paradinas, M. Panighel, G. Ceballos, S. O. Valenzuela, D. Peña, A. Mugarza, *Science* **2018**, *360*, 199–203, https://doi.org/10.1126/science.aar2009.

[20] G. Galeotti, F. De Marchi, E. Hamzehpoor, O. MacLean, M. R. Rao, Y. Chen, L. V. Besteiro, D. Dettmann, L. Ferrari, F. Frezza, P. M. Sheverdyaeva, R. Liu, A. K. Kundu, P. Moras, M. Ebrahimi, M. C. Gallagher, F. Rosei, D. F. Perepichka, G. Contini, *Nat. Mater.* **2020**, *19*, 874–880.

[21] Q. Fan, L. Yan, M. W. Tripp, O. Krejčí, S. Dimosthenous, S. R. Kachel, M. Chen, A. S. Foster, U. Koert, P. Liljeroth, J. M. Gottfried, *Science* **2021**, *372*, 852–856, https://doi.org/10.1126/science.abg4509.

[22] B. Cirera, N. Giménez-Agulló, J. Björk, F. Martínez-Peña, A. Martin-Jimenez, J. Rodriguez-Fernandez, A. M. Pizarro, R. Otero, J. M. Gallego, P. Ballester, J. R. Galan-Mascaros, D. Ecija, *Nat. Commun.* **2016**, *7*, 11002, https://doi.org/10.1038/ncomms11002.

[23] E. Pérez-Elvira, A. Barragán, Q. Chen, D. Soler-Polo, A. Sánchez-Grande, D. J. Vicent, K. Lauwaet, J. Santos, P. Mutombo, J. I. Mendieta-Moreno, B. De La Torre, J. M. Gallego, R. Miranda, N. Martín, P. Jelínek, J. I. Urgel, D. Écija, *Nature Synthesis* **2023**, *2*, 1159–1170, https://doi.org/10.1038/s44160-023-00390-8.

[24] E. Pérez-Elvira, A. Barragán, A. Gallardo, J. Santos, C. Martín-Fuentes, K. Lauwaet, J. M. Gallego, R. Miranda, H. Sakurai, J. I. Urgel, J. Björk, N. Martín, D. Écija, *Angew. Chem. Int. Ed.* **2025**, *64*, e202414583, https://doi.org/10.1002/anie.202414583.

[25] J. Roncali, *Chem. Rev.* **1992**, *92*, 711–738, https://doi.org/10.1021/cr00012a009.

[26] J. Casado, R. Ponce Ortiz, J. T. López Navarrete, *Chem. Soc. Rev.* **2012**, *41*, 5672, https://doi.org/10.1039/c2cs35079c.

[27] G. Barbarella, M. Melucci, G. Sotgiu, *Adv. Mater.* **2005**, *17*, 1581–1593, https://doi.org/10.1002/adma.200402020.

[28] M. E. Cinar, T. Ozturk, *Chem. Rev.* **2015**, *115*, 3036–3140, https://doi.org/10.1021/cr500271a.

[29] G. Turkoglu, M. E. Cinar, T. Ozturk, *Topics in Current Chemistry* **2017**, *375*, 84, https://doi.org/10.1007/s41061-017-0174-z.

[30] R. Shah, P. K. Verma, *Chem. Cent. J.* **2018**, *12*, 137, https://doi.org/10.1186/s13065-018-0511-5.

[31] S. Ye, V. Lotocki, H. Xu, D. S. Seferos, *Chem. Soc. Rev.* **2022**, *51*, 6442–6474, https://doi.org/10.1039/D2CS00139J.

[32] W. Wu, Y. Liu, D. Zhu, *Chem. Soc. Rev.* **2010**, *39*, 1489–1502, https://doi.org/10.1039/B813123F.

[33] L. Liu, X. Miao, T. Shi, X. Liu, H.-L. Yip, W. Deng, Y. Cao, *Nanoscale* **2020**, *12*, 18096–18105, https://doi.org/10.1039/D0NR04529B.

[34] L. Cardenas, R. Gutzler, J. Lipton-Duffin, C. Fu, J. L. Brusso, L. E. Dinca, M. Vondráček, Y. Fagot-Revurat, D. Malterre, F. Rosei, D. F. Perepichka, *Chem. Sci.* **2013**, *4*, 3263, https://doi.org/10.1039/c3sc50800e.

[35] G. Reecht, H. Bulou, F. Scheurer, V. Speisser, B. Carrière, F. Mathevet, G. Schull, *Phys. Rev. Lett.* **2013**, *110*, 056802, https://doi.org/10.1103/PhysRevLett.110.056802.

[36] X.-Y.u Zhang, J.-H. Fu, Z.-Q. Chen, W.-W. Gong, Y. Wang, L.i-X. Kang, Y. Zhao, C.-H. Shu, D.-Y. Li, P.-N. Liu, *ACS Nano* **2025**, *19*, 16545–16553, https://doi.org/10.1021/acsnano.4c18959.

[37] T. Michnowicz, B. Borca, R. Pétuya, V. Schendel, M. Pristl, I. Pentegov, U. Kraft, H. Klauk, P. Wahl, P. Mutombo, P. Jelínek, A. Arnau, U. Schlickum, K. Kern, *Angew. Chem. Int. Ed.* **2020**, *59*, 6207–6212, https://doi.org/10.1002/anie.201915200.

[38] B. Borca, T. Michnowicz, R. Pétuya, M. Pristl, V. Schendel, I. Pentegov, U. Kraft, H. Klauk, P. Wahl, R. Gutzler, A. Arnau, U.

Schlickum, K. Kern, *ACS Nano* **2017**, *11*, 4703–4709, https://doi.org/10.1021/acsnano.7b00612.
[39] L. E. Dinca, C. Fu, J. M. Macleod, J. Lipton-Duffin, J. L. Brusso, C. E. Szakacs, D. Ma, D. F. Perepichka, F. Rosei, *ACS Nano* **2013**, *7*, 1652–1657, https://doi.org/10.1021/nn305572s.
[40] P. Ji, D. Dettmann, Y.-H. Liu, G. Berti, N. Preetha Genesh, D. Cui, O. Maclean, D. F. Perepichka, L. Chi, F. Rosei, *ACS Nano* **2022**, *16*, 6506–6514, https://doi.org/10.1021/acsnano.2c00831.
[41] S. Kawai, V. Haapasilta, B. D. Lindner, K. Tahara, P. Spijker, J. A. Buitendijk, R. Pawlak, T. Meier, Y. Tobe, A. S. Foster, E. Meyer, *Nat. Commun.* **2016**, *7*, 12711, https://doi.org/10.1038/ncomms12711.
[42] A. Shiotari, T. Nakae, K. Iwata, S. Mori, T. Okujima, H. Uno, H. Sakaguchi, Y. Sugimoto, *Nat. Commun.* **2017**, *8*, 16089, https://doi.org/10.1038/ncomms16089.
[43] A. Riss, S. Wickenburg, P. Gorman, L. Z. Tan, H.-Z. Tsai, D. G. De Oteyza, Y.-C. Chen, A. J. Bradley, M. M. Ugeda, G. Etkin, S. G. Louie, F. R. Fischer, M. F. Crommie, *Nano Lett.* **2014**, *14*, 2251–2255, https://doi.org/10.1021/nl403791q.
[44] A. Riss, A. P. Paz, S. Wickenburg, H.-Z. Tsai, D. G. De Oteyza, A. J. Bradley, M. M. Ugeda, P. Gorman, H. S. Jung, M. F. Crommie, A. Rubio, F. R. Fischer, *Nat. Chem.* **2016**, *8*, 678–683, https://doi.org/10.1038/nchem.2506.
[45] D. G. de Oteyza, P. Gorman, Y.-C. Chen, S. Wickenburg, A. Riss, D. J. Mowbray, G. Etkin, Z. Pedramrazi, H.-Z. Tsai, A. Rubio, M. F. Crommie, F. R. Fischer, *Science* **2013**, *340*, 1434–1437, https://doi.org/10.1126/science.1238187.
[46] K. Biswas, Q. Chen, S. Obermann, J.i Ma, D. Soler-Polo, J. Melidonie, A. Barragán, A. Sánchez-Grande, K. Lauwaet, J. M. Gallego, R. Miranda, D. Écija, P. Jelínek, X. Feng, J. I. Urgel, *Angew. Chem. Int. Ed.* **2024**, *63*, e202318185, https://doi.org/10.1002/anie.202318185.
[47] Q. Chen, M. Di Giovannantonio, K. Eimre, J. I. Urgel, P. Ruffieux, C. A. Pignedoli, K. Müllen, R. Fasel, A. Narita, *Macromol. Chem. Phys.* **2023**, *224*, 2300345, https://doi.org/10.1002/macp.202300345.
[48] Q. Sun, B. V. Tran, L. Cai, H. Ma, X. Yu, C. Yuan, M. Stöhr, W. Xu, *Angew. Chem. Int. Ed.* **2017**, *56*, 12165–12169, https://doi.org/10.1002/anie.201706104.
[49] A. Sánchez-Grande, J. I. Urgel, A. Cahlík, J. Santos, S. Edalatmanesh, E. Rodríguez-Sánchez, K. Lauwaet, P. Mutombo, D. Nachtigallová, R. Nieman, H. Lischka, B. d. l. Torre, R. Miranda, O. Gröning, N. Martín, P. Jelínek, D. Écija, *Angew. Chem. Int. Ed.* **2020**, *59*, 17594–17599, https://doi.org/10.1002/anie.202006276.
[50] C. Martín-Fuentes, J. I. Urgel, S. Edalatmanesh, E. Rodríguez-Sánchez, J. Santos, P. Mutombo, K. Biswas, K. Lauwaet, J. M. Gallego, R. Miranda, P. Jelínek, N. Martín, D. Écija, *Chem. Commun.* **2021**, *57*, 7545–7548, https://doi.org/10.1039/D1CC02058G.
[51] J. I. Urgel, A. Sánchez-Grande, D. J. Vicent, P. Jelínek, N. Martín, D. Écija, *Adv. Mater.* **2024**, *36*, 2402467, https://doi.org/10.1002/adma.202402467.
[52] L. Gross, F. Mohn, N. Moll, B. Schuler, A. Criado, E. Guitián, D. Peña, A. Gourdon, G. Meyer, *Science* **2012**, *337*, 1326–1329, https://doi.org/10.1126/science.1225621.
[53] P. Hapala, G. Kichin, C. Wagner, F. S. Tautz, R. Temirov, P. Jelínek, *Phys. Rev. B* **2014**, *90*, 085421, https://doi.org/10.1103/PhysRevB.90.085421.
[54] I. Novak, *Journal of Photochemistry and Photobiology A: Chemistry* **2024**, *447*, 115222, https://doi.org/10.1016/j.jphotochem.2023.115222.
[55] A. Konishi, T. Fujiwara, N. Ogawa, Y. Hirao, K. Matsumoto, H. Kurata, T. Kubo, C. Kitamura, T. Kawase, *Chem. Lett.* **2010**, *39*, 300–301, https://doi.org/10.1246/cl.2010.300.

Manuscript received: September 23, 2025
Revised manuscript received: December 16, 2025
Manuscript accepted: December 17, 2025
Version of record online: December 31, 2025